Magnetic Interaction in Solvent-free DPPH and DPPH-Solvent Complexes

Teruaki FUJITO†

Department of Chemistry, Faculty of Science, Kyoto University, Sakyo-ku, Kyoto 606

(Received December 19, 1980)

Magnetic interaction in solvent-free DPPH and DPPH–solvent complexes has been studied by means of measurements of the magnetic susceptibility, the proton magnetic resonance, and the low-field ESR at very low temperatures. The susceptibility of solvent-free DPPH shows a round maximum at 11 K, and then it decreases with a lowering of the temperature, no ordered state being observed. The DPPH–benzene (1 : 1) complex shows a round maximum of susceptibility at 0.65 K and antiferromagnetic ordering at about 0.40 K. The DPPH–CCl_4 (4 : 1) complex shows a curious temperature dependence of the susceptibility, which is interpreted in terms of a two-magnetic sublattice model; one sublattice is in the singlet spin state, while the other is in the paramagnetic state at low temperatures except below 0.45 K. Pair interaction is dominant both solvent-free DPPH and in solvent complexes of DPPH. A theoretical approach to the ordered state of DPPH–benzene is given by taking the inter-pair interaction into account.

Recently many studies have been made of the magnetic properties of some organic stable free radicals, such as 4-hydroxy-2,2,6,6-tetramethyl-1-piperidinoxyl (TANOL), diphenyl nitroxide (DPNO) and 1,3-bis-(biphenyl-2,2′-diyl)-2-phenylallyl (BDPA).[1,2] It has been found that the linear-chain interaction is dominant in these radicals. 2,2-Diphenyl-1-picrylhydrazyl (DPPH) is a well known, stable, organic free radicals, and its magnetic properties have been investigated by many workers using various techniques.[3-5] However, the results obtained by different workers have not been consistent with each other. For example, the results of NMR by Karimov and Schegolev[5] were different from those reported by Anderson, Pake, and Tuttle.[4] In 1965, Weil and Anderson[6] reported that there are three different crystal forms for the group of solvent-free DPPH and DPPH-solvent complexes (this group will be abbreviated as DPPHs hereafter). Subsequent X-ray investigations by Williams showed that there are indeed three types of crystal structures for DPPHs.[7] Hence, the complication of the magnetic properties of DPPHs is probably due to the differences in the crystal structures of the samples used by different workers. In order to understand the magnetism of DPPHs, it is, therefore, important to examine the relation between magnetism and crystal structure.

Previously, we measured the magnetic susceptibilities of several DPPHs samples obtained by recrystallization from different solvents.[8] The results showed that the magnetic susceptibilities are also classified into three types in accordance with the structure types reported by Williams. In this paper, the author will report the results of powder-magnetic-susceptibility, NMR, and ESR measurements of DPPH recrystallized from ether (hereafter abbreviated as free DPPH), DPPH–benzene (1 : 1) complex (DPPH–Bz), and DPPH–CCl_4 (4 : 1) complex (DPPH–1/4CCl_4), in addition to the single-crystal-susceptibility measurements of DPPH–Bz; he will also discuss the types of magnetic interactions existing in the different types of crystals.

Here let us review the crystal structure of DPPHs before we proceed to the analysis of the magnetic properties. In the free DPPH, DPPH molecules are more closely packed (d=1.485) than in any other crystals of DPPH–solvent complexes. The crystal parameters of the free DPPH have been reported, but their precise structure has not yet been established. The crystal structure of DPPH–Bz, on the other hand, was precisely determined.[7] In this case, DPPH molecules align face-to-face to form a chain along the a-axis (Fig. 1a). A DPPH molecule at site "A" is 0.776 nm from the adjacent DPPH molecule at the same site along the a-axis. The DPPH molecules at site "B" are in a similar situation. The DPPH molecules at site "A" and site "B" make an alternative array. The nearest distance between the centers of their N–N bonds is about 0.85 nm. Two phenyl rings, the α phenyl of A_0 and the β phenyl of B_0 in Fig. 1b, however, have the nearest carbon-carbon distance of 0.372 nm. Recently, the crystal structure of the DPPH–acetone (4 : 1) complex, considered to be very similar to that of DPPH–

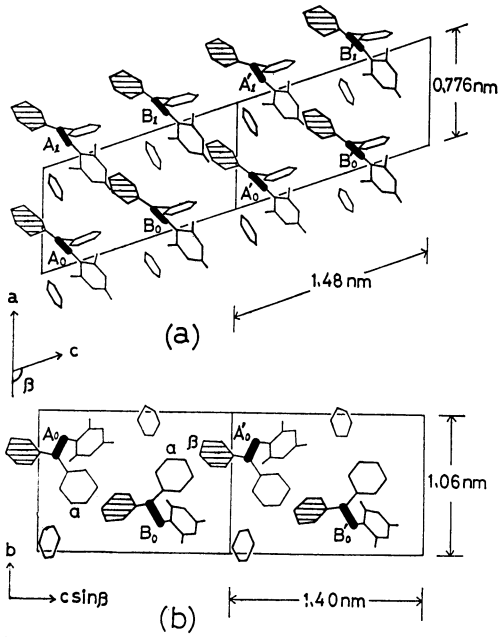

Fig. 1. The crystal structure of DPPH–Bz projected on the ac-plane(a) and on the bc-plane(b) from the Williams' work. N–N bonds are shown by rods. A and B mean DPPH molecules in site "A" and site "B", respectively. α represents α-phenyl rings and β does β-phenyl rings (shaded portion).

† Present address: JEOL Ltd., Akishima, Tokyo 196.

$1/4CCl_4$, was reported by Kiers *et al.*[9] This crystal has a hole with a diameter of at least 0.6 nm, which an acetone molecule possibly occupies, and four DPPH molecules in a unit cell ($z=4$). The four DPPH molecules are located in two different crystallographic sites. Two of the four DPPH molecules in the unit cell are related to each other by an inversion center and are close together, with a distance of only 0.595 nm between the centers of their N–N bonds. These molecules surround the hole mentioned above, so that the molecules have a relatively large freedom of motion. On the other hand, the other two molecules are separated by a distance of 0.692 nm between the centers of their N–N bonds. However, the nearest two phenyl rings of the latter lie parallel to each other at a carbon distance of 0.393 nm. Solvent–acetone molecules are randomly distributed in the holes which make channels along the c-axis. The number of the acetone molecules is about one-fourth that of the DPPH molecules.

These DPPHs show different magnetic properties. The susceptibility of DPPH–Bz and free DPPH were explained by a pair model of localized spins (localized model).[8,10,11] The DPPH–$1/4CCl_4$ complex shows a curious magnetic susceptibility which gives two Weiss constants, θ_{high} (above 30 K) and θ_{low} (below 4.2 K). The spin concentration in the low-temperature region (below 4.2 K) is half of that in the high-temperature region (above 30 K). In order to interpret this phenomenon, Duffy and Strandberg[9] proposed a "two-sublattice model," one featuring the coexistence of strong and weak pair interactions between the electron spins localized on the DPPH molecules in the crystal. On the other hand, Fedders and Kommandeur[12] applied a "narrow-band model" to explain the magnetic susceptibility of the DPPH complexes. They assumed a delocalization of unpaired electrons throughout the crystal, resulting in the formation of an energy band of the electrons.

In this paper, the present author tries to answer the following questions on the basis of the results of his magnetic measurements: (1) Which models are suitable to explain the magnetic behavior of the DPPHs crystals? (2) What types of magnetic interactions are dominant in these crystals? (3) How do the solvent molecules affect the magnetic properties of the DPPH–solvent complexes?

Experimental

The samples were prepared by the oxidation of 2,2-diphenyl-1-picryl-hydrazine($DPPH_2$) with PbO_2 in extra pure diethyl ether, benzene, carbon tetrachloride, carbon disulfide, or chloroform solutions; they were then recrystallized several times using the same solvents. It was confirmed by the elementary analyses and preliminary X-ray analyses that the free DPPH and DPPH–solvent complexes can be classified into three groups with the different, definite crystal structures (I, III, and DPPH–Bz) reported in Williams' paper.[7] Free DPPH has the same crystal structures as that of DPPH(I), while DPPH–Bz has the crystal structure identified by him. The crystal parameters of the complexes of DPPH with CS_2, CCl_4, and $CHCl_3$ are very close to those of DPPH(III) in Williams' paper[7] and those of DPPH(IIIa) in Kiers' paper.[9]

Magnetic-susceptibility(χ) measurements of polycrystalline samples were carried out with a magnetic torsion balance at temperatures between 1.2 K and 4.2 K and with a bridge method at the temperatures obtained by the adiabatic demagnetization described below. The measurement of the anisotropy of the magnetic susceptibility in DPPH–Bz was carried out in order to determine the phase-transition temperature (T_N) to an antiferromagnetic state using a single crystal of 1.34g in the adiabatic-demagnetization temperature region. Single crystals of free DPPH and DPPH–$1/4CCl_4$ were too small for us to measure the anisotropy of χ. The data obtained by the torsion balance above 1.7 K have been corrected for diamagnetism by the use of Pascal's constants. The data at the adiabatic-demagnetization temperatures were fitted to the data measured by the torsion balance at 4.22 K. The adiabatic demagnetization was carried out following the standard method. Samples were mixed with a high-vacuum diffusion oil and Apiezone-N-grease, and placed in contact with a coolant of chromium potassium alum (Cr–K–Alum) through 3000 Cu-formal wires. The temperatures were determined from the paramagnetic susceptibility of Cr–K–Alum to temperature measurement; this substance was thermally linked by copper wires to the samples. The temperature gradient between the sample and the coolant was calibrated by comparing the susceptibility of the coolant with that of Cr–K–Alum mixed with diamagnetic $DPPH_2$ at the same position. The temperatures, T^*, thus obtained were corrected to thermodynamic ones, T, by the use of T^*-*vs.*-T table.[13]

In order to study the paramagnetic shift, ^{1}H-NMR resonance (PMR) measurements were performed on powder samples (*ca.* 1 g), using Robinson and Pound-Knight-Watkins-type spectrometers operating at 12—40 MHz in the tempera-

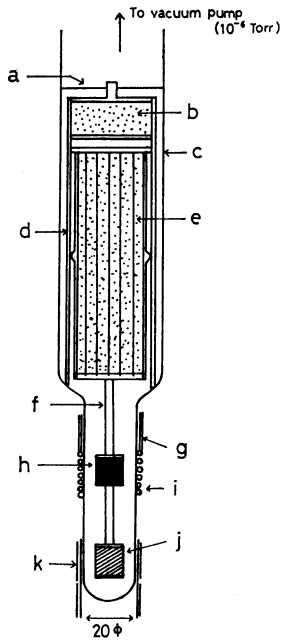

Fig. 2. Sample cell for low-field ESR in adiabatic demagnetization temperature region.
(a) Stainless steel spring, (b) heat guard; Mn-Tutton salt, (c) 40 mmϕ glass tube, (d) polycarbonate sample cell, (e) coolant; Cr–K–Alum, (f) Cu rod for heat link, (g) 3 mmϕ stainless steel tube for Lecher line, (h) sample, (i) RF coil (1.5 mmϕ, 6 turns), (j) Cr–K–Alum for thermometer, (k) coil for temperature measurement.

ture range of 1.3—77 K. Low-field ESR measurements were carried out with a Kushida-type spectrometer[14] with 80 Hz field modulation to confirm the presence of the antiferromagnetic state and T_N. The sample cell for low-field ESR in the adiabatic-demagnetization-temperature region is shown in Fig. 2. The field-modulation power and radio-frequency power were minimized to prevent sample heating.

Results

Magnetic Susceptibility. The data were analyzed with the isolated-pair model and also the interacting-pair model to be discussed later. The susceptibility in the isolated-pair model[15] is accurately given by:

$$\chi = \frac{N'g^2\beta^2S(S+1)}{3kT}\frac{1}{1+1/3\exp(\delta/kT)}, \quad (1)$$

where $\delta=2|J|$ and where N' is the number of spin pairs with $S=1$, which is half the Avogadro number. Here, δ means the singlet-triplet energy separation for the electron-spin pairs. The exponential function in Eq. 1 can be expanded in the series of δ/kT; the high-temperature approximation for Eq. 1 is given as follows:

$$\chi = \frac{N'g^2\beta^2S(S+1)}{4k(T+\delta/4k)} = \frac{C'}{T+\theta'}, \quad (2)$$

where $C'=N'g^2\beta^2S(S+1)/4k$ and $\theta'=\delta/4k$. Thus, the susceptibility in the pair model shows the same form as that of the Curie-Weiss law at high temperatures where $T\gg\delta/k$. Figure 3 shows the molar susceptibilities of DPPHs, with the theoretical curves calculated using Eq. 1.

Free DPPH: Free DPPH showed a magnetic behavior which can be well explained by the pair model with $\delta/k=17.6$ K at temperatures down to 5 K. In the temperature region between 1.8 and 2.5 K, on the other hand, a paramagnetic contribution to the susceptibility corresponding to a spin concentration of 2.5% was observed (see Fig. 3). From the comparison with

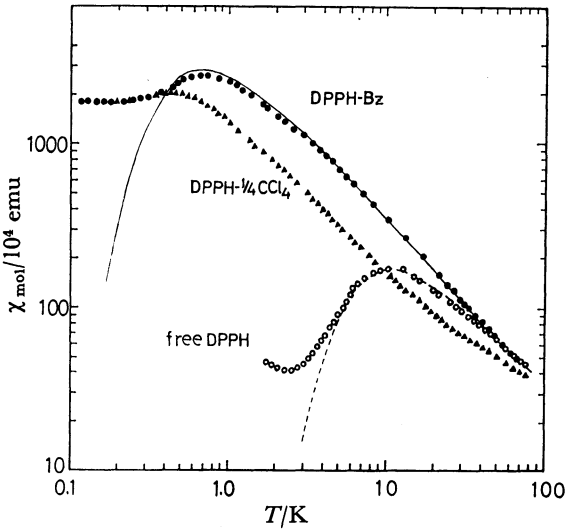

Fig. 3. Powder magnetic susceptibilities of free DPPH and DPPH solvent complexes, where 1 χ_{mol} (emu)= $4\pi\chi_{mol}$ (SI). Solid line : pair model curve with $\delta/k=$ 1.04 K. Dotted line : pair model curve with $\delta/k=$ 17.6 K.

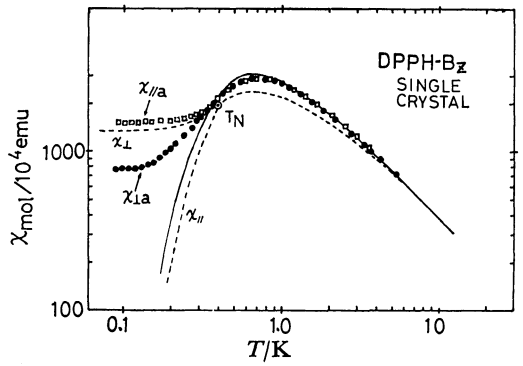

Fig. 4. Anisotropy of the magnetic susceptibility of DPPH–Bz single crystal. Solid line represents the pair model curve with $\delta/k=1.04$ K, and dotted line is the interacting-pair model for $\kappa=1.3$ (Ohya's model). $\chi_{//}$ and $\chi_\perp$ denote the susceptibilities parallel and perpendicular to the easy axis, respectively.

the paramagnetic shifts in the PMR spectra described below, it is concluded that the susceptibility increase below 2.5 K is due to an isolated paramagnetic "impurity."

DPPH–Bz: The susceptibility of DPPH–Bz reached a maximum χ_{max} at about 0.65 K and remained constant below 0.3 K. The data above 0.40 K are better fitted to the pair model with $\delta/k=1.04$ K than to other models, such as the linear-chain model. Figure 4 shows the anisotropy of the susceptibility in a DPPH–Bz single crystal. The squares (□) and filled circles (●) in the figure indicate the observed susceptibility along the a-axis ($\chi_{//a}$) and the directions perpendicular to the a-axis ($\chi_{\perp a}$) respectively; they show the anisotropy of the susceptibility below 0.40 K. These data suggest an antiferromagnetic ordering at about 0.40 K in the DPPH–Bz.

DPPH–1/4CCl_4: This sample is characterized by two Weiss constants, $\theta_{high}=-26$ K and $\theta_{low}=-0.3$ K, in the temperature ranges above 30 K and below 4.2 K respectively, which were obtained from a comparison of the experimental susceptibility and the Curie-Weiss law in Eq. 2. The spin concentration, C, in the low-temperature region (below 4.2 K) is about half the high-temperature one (above 30 K). In the intermediate region (4.2—30 K), θ and C gradually changed. The susceptibility increased with a lowering of the temperature from 1.7 K down to 0.45 K and remained constant below 0.45 K. The constant susceptibility, probably due to spin ordering below 0.45 K, had a value similar to that of the DPPH–Bz complex. In the high-temperature region (above 30 K), the best fit for the pair model is obtained by assuming δ/k(high)= 96 K. The remaining unpaired spins at temperatures between 4.2 and 0.45 K show an ordinary paramagnetic behavior, following the Curie-Weiss law with the Weiss constant $\theta=-0.3$ K.

A summary of the susceptibility data is given in Table 1, where C is the spin concentration obtained by comparing the observed and theoretical Curie constants.

Proton Magnetic Resonance. In the case of the powder samples, the PMR line-width (ΔH_i) is proportional to both the resonance field for the i-th proton, H_i,

TABLE 1. SUMMARY OF THE MAGNETIC SUSCEPTIBILITY DATA

Sample	T_{max} [a] / K	χ_{max} [b]	C	θ / K	δ / kK	$\lvert J\rvert$ / kK	T_N / K
Free DPPH	11.0	175	0.98	−10.0	17.6	8.8	Unknown
DPPH-Bz	0.65	2900	1.00	−0.5	1.04	0.52	0.40
DPPH-1/4CCl_4	60 0.45	15 2000	0.86 [c] 0.44 [d]	−26.0 [c] −0.3 [d]	96 [c] —	48 [c] —	Unknown

a) Temperature of χ_{max}. b) Maximum susceptibility in 10^{-4} emu/mol. c) Determined by measurements above 30 K. d) Determined by measurements below 4.2 K.

and the magnetic susceptibility, χ, because of the proton-electron dipolar interaction. The paramagnetic shift (δH_i) is also proportional to χ and H_i, as is given by:

$$\delta H_i = H_i - H_0 = -\frac{a_i \chi H_i}{g_N \beta_N}, \quad (3)$$

where H_0 is the resonance field for the free proton and where a_i is the hyperfine constant of the i-th proton. For $T \gg \delta/k$, this equation can be approximated as:

$$\delta H_i \cong \frac{-5.2 \nu_i a_i}{T+\theta} \quad (4)$$

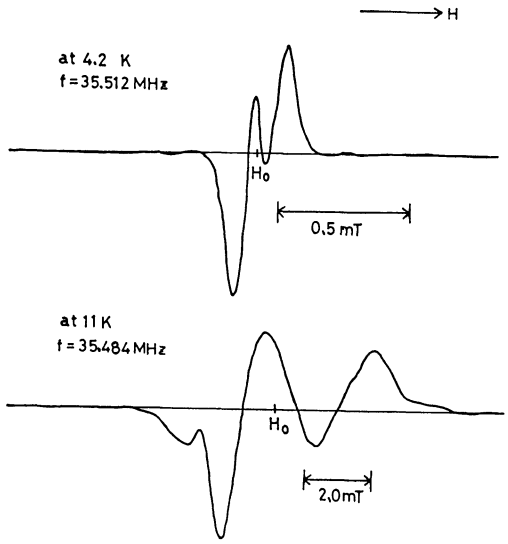

Fig. 5. PMR spectra of free DPPH at low temperatures.

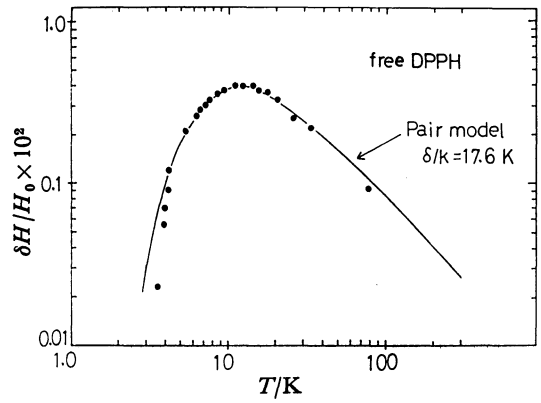

Fig. 6. Temperature dependence of the relative paramagnetic shift of free DPPH.

where ν_i is the observed resonance frequency in MHz and where $2\pi\nu_i = \gamma_N H_i$. Therefore, one can determine χ and the microscopic behavior of the compounds by measuring the temperature dependence of δH_i and ΔH_i.

Free DPPH: Figure 5 shows the PMR-derivative spectra of free DPPH at 4.2 and 11 K. At about 11 K, where the susceptibility shows χ_{max}, four lines were resolved, the ratio of the integrated line intensities being 2 : 4 : 3 : 3. It should be noted that the unshifted line does not appear at these temperatures. The distance between the inner two lines of the spectra, δH, has the same temperature dependence as that of the observed susceptibility, and agrees well with that predicted by the pair model with $\delta/k = 17.6$ K (Fig. 6). The pair-model curve in Fig. 6 was fitted to the experimental results so that its maximum value coincided with the experimental one at 11 K. In spite of an increase in the static magnetic susceptibility below 2.5 K, the spectra did not show any shifted lines down to 1.2 K, as in Verlinden's work.[16] It can be easily deduced from Eq. 3 that the disappearance of the shift leads to the decrease in χ. Therefore, the susceptibility increase below 2.5 K shown in Fig. 3 is due to isolated paramagnetic "impurity" spins, the concentration being about 2.5%.

DPPH-Bz: The PMR spectra of DPPH-Bz show five lines at 4.2 K, as given in a previous paper.[4] The intensity ratio of the five lines is about 2 : 4 : 6 : 3 : 3. This ratio is consistent with the number of protons at five different positions in DPPH-Bz: *i.e.*, two protons in metapicryl, four protons in metaphenyl, six protons in benzene, three protons at the ortho and para positions in α phenyl, and three protons at the ortho and para positions in β phenyl.[17] When the reciprocal of the paramagnetic shifts, δH_i, is plotted as a function of the temperature, the Weiss constant of $\theta = -0.5$ K is obtained by extrapolation to the absolute zero degree. This θ value is in good agreement with that obtained from the susceptibility measurements. As the temperature is lowered or frequency is increased, the shifted lines become broader and split further. The broadening of the lines is roughly proportional to χ. The central line due to benzene protons is easily saturated at 1.5 K, because the spin-lattice relaxation time, T_1, of the diamagnetic benzene protons is longer than those of the paramagnetic DPPH protons.

DPPH-1/4CCl_4: The PMR spectra of DPPH-1/4CCl_4 below 20 K showed a strong unshifted line which is easily saturated at 1.5 K, in addition to four weak, shifted lines (two high-field and two low-field shifted lines), as was shown in Karimov's paper.[5] Above 20 K,

four shifted lines coalesced into a broad central line. The intensity ratio of the unshifted central line to the sum of the four shifted lines at 18.082 MHz was determined to be 2.5 : 1 from the PMR absorption spectra at 4.2 K. The intensity of the central line increased as the frequency became higher. The unshifted line can be attributed not to the protons of the DPPH molecule in the paramagnetic state, but to the protons of DPPH in the singlet state.[16] The relative shift for this sample is somewhat larger than that for DPPH–Bz. The following results were obtained from the reciprocal plot of the paramagnetic shift *versus* the temperature. In the lower temperature region (below 4.2 K), the Weiss constant $\theta_{low}=-0.2$ K is in agreement with that obtained from the susceptibility measurement.

Low-field ESR. In order to confirm the long-range ordering observed by the anisotropy of χ for DPPH–Bz, low-field ESR measurements were carried out at 74.4 MHz in the range from 0.27 K to 4.2 K. The derivative spectra are shown in Fig. 7. The $g=2$ signal intensity decreased rapidly below 0.6 K. The line-width, ΔH_{pp}, increased with a lowering of the temperature and then diverged between 0.46 and 0.42 K. (Fig. 8) Below 0.42 K, the $g=2$ resonance became very small, and the $g=4$ resonance due to forbidden dipolar transition became dominant.[18] The rapid increase in the line-width observed in the paramagnetic region near 0.42 K is interpreted as follows: the critical fluctuation sets in the spin system and makes the exchange correlation time, τ_e, long[19] thus reducing the extent of exchange narrowing of the ESR line-width. Then, long-range ordering occurs at about 0.40 K. The transition temperature to the antiferromagnetic state (0.43 ± 0.03 K) is consistent with that determined from the magnetic-susceptibility measurements for a single-crystal sample.

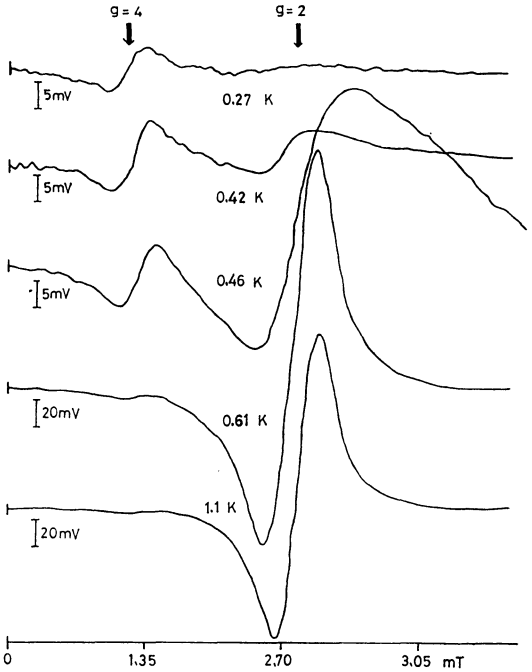

Fig. 7. Low-field ESR spectra of DPPH–Bz at 74.4 MHz.

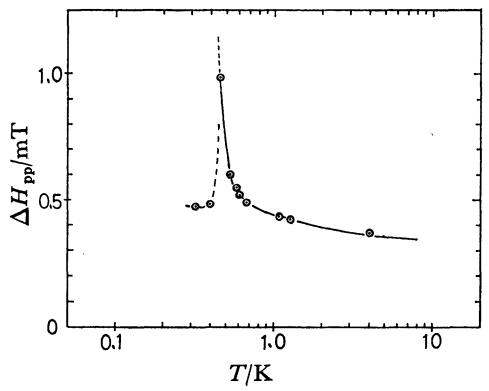

Fig. 8. Temperature dependence of low-field ESR ($g=2$) line-width of DPPH–Bz.

Discussion

Magnetic Interaction in the Paramagnetic State. From the results of the magnetic susceptibility shown in Fig. 3, it can easily be understood that, in the DPPH–solvent complexes, solvent molecules play an important part in constructing a spatial configuration of the magnetic moments. Different solvents form free DPPH and different solvent complexes with certain crystal structures. Therefore, the type and the intensity of magnetic interaction depend on the solvent used for preparing the crystal.

In the free DPPH, DPPH molecules are most closely packed in the crystal ($d=1.485$). The susceptibility results show that every two molecules make pairs with a strong antiferromagnetic exchange interaction ($J/k=-8.8$ K) and fall into a singlet ground state at low temperatures below about 3 K. The results of the paramagnetic shift in PMR spectra support this model. No fall in the PMR intensity was observed in the free DPPH below 3 K, at which point the paramagnetic shift lines are coalesced into an unshifted single line, while a sudden decrease in PMR intensity was observed in the BDPA and TANOL radicals in the vicinity of their antiferromagnetic transition.[20,21] In the low-field ESR measurements, a maximum of the line-width was observed in DPPH–Bz near the Néel temperature, while no such maximum was observed in the free DPPH. From these results, one can conclude that the magnetic properties of the free DPPH are characterized by the isolated-pair model.

In the case of DPPH–Bz, the powder magnetic susceptibility in Fig. 3 and that as well as the heat capacity measured by Duffy *et al.*[11] show that the pair interaction is rather dominant in this crystal. The pair interaction, however, does not lead to any long-range ordering. Therefore, some inter-pair exchange interaction must be taken into account in order to explain the antiferromagnetic ordering. Duffy *et al.* proposed the exchange paths for DPPH–Bz described below in order to explain the magnetic susceptibility in the paramagnetic region: DPPH molecules which are 0.776 nm apart from each other along the a-axis are considered to form a chain along this axis from the crystallographic point of view (Fig. 1a), suggesting the existence of linear-chain-type interaction along this axis.

In a DPPH molecule, the unpaired electron is not localized on a N–N bond, about 30% of it being distributed on the phenyl and picryl rings.[22] Therefore, the exchange interaction between the unpaired electron on Site "A" and on Site "B" will take place dominantly through the overlap of the $2p\pi$-orbitals on the adjacent α and β phenyl rings. (Fig. 1b) This interpretation is reasonable if we take the crystal structure into account. However, their heat capacity and susceptibility measurements were limited to the paramagnetic region, and there was no mention of the antiferromagnetic transition. Below we will discuss the phase transition using the interacting-pair model based on the interpretation of the exchange path mentioned above.

DPPH–1/4CCl_4 shows more complicated magnetic behavior. The magnetic susceptibility results have been explained by both the two-sublattice model and the narrow-band model. However, the PMR spectra can be analyzed in terms of the coexistence of weakly and strongly coupled spin pairs, supporting the two-sublattice model proposed by Duffy *et al.* This excludes the narrow-band model. The following exchange mechanism is suggested from the point of view of the two-sublattice model. DPPH–1/4CCl_4 has one CCl_4 molecule and four DPPH molecules in a unit cell. The two DPPH molecules are close together (0.595 nm) and are mutually coupled with a strong exchange interaction. They form singlet spin pairs at higher temperatures compared with free DPPH. On the other hand, the other two weakly coupled DPPH molecules (0.692 nm apart) interact with each other with some weak exchange interactions through both paths between nearest N–N bonds and between nearest phenyl rings, which may trigger an antiferromagnetic ordering of unpaired spins below 0.9 K.[23]

Phase Transition to Antiferromagnetic State. An antiferromagnetic ordering of DPPH–Bz was suggested by Prokhorov and Fedrov from the disappearance of the low-field ESR signal near 0.18 K.[24] In the present work, the low-field ESR signal disappeared at 0.43 ± 0.03 K, below which point the magnetic susceptibility of a powder sample approaches a finite constant value with a decrease in the temperature. In addition, the single crystal shows magnetic anisotropy below 0.40 K, as is shown in Fig. 4. All of these data support the appearance of an antiferromagnetic ordering about 0.40 K. The Néel temperature, T_N, is higher than that given by Prokhorov and Fedrov. As has been described already, the paramagnetic susceptibility of DPPH–Bz is rather well described by the isolated-pair model, although linear-chain interaction can be expected to be dominant from its crystallographic data. Duffy, Strandburg, and Deck reported the susceptibility and heat capacity of DPPH–Bz from 0.4 K up to room temperature, but neither the linear-chain model nor the quadratic-net Heisenberg model gives a satisfactory explanation of their data. The pair interaction, J, however, cannot cause a long-range ordering. Therefore, in order to explain the long-range ordering of a spin-pair system, inter-pair interaction must be considered. We try to explain the long-range ordering temperature and the magnetic behavior, in both paramagnetic and antiferromagnetic regions, by using the following model as a first-order approximation. This model is a modified version of Oguchi's "improved molecular field theory of the antiferromagnet,"[25] the details of which were recently described by Ohya-Nishiguchi.[26]

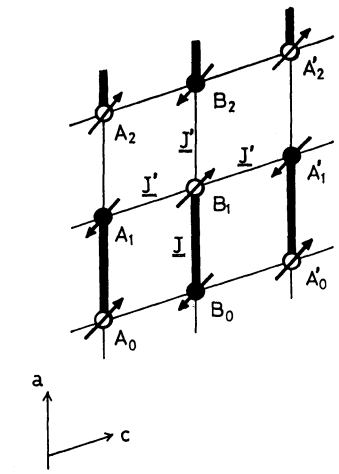

Fig. 9. Interacting-pair model for DPPH–Bz. The positions of DPPH molecules are projected in the ac-plane. J and J' represent intra-pair and averaged inter-pair interactions, respectively.

Assuming a spin pair i-j with intra-pair exchange interaction, J, having other exchange interactions with their neighboring spin pairs, averaged as $J'(|J'|<|J|)$, as is shown in Fig. 9. J' is treated as a kind of molecular field. For such a spin system, a two-body Hamiltonian is given by the following equation:

$$\begin{aligned} \mathcal{H} &= 2|J|(\boldsymbol{S}_i\cdot\boldsymbol{S}_j) + aS_i^z + bS_j^z \\ a &= 2|J'|Z'(-\langle S^z\rangle+\langle\delta S^z\rangle) - g\mu H^z \\ b &= 2|J'|Z'(\langle S^z\rangle+\langle\delta S^z\rangle) - g\mu H^z, \end{aligned} \tag{4}$$

where Z' is the number of the nearest interaction paths of i-spin with all neighboring spins except the j-spin and is equal to three in the case of Fig. 9. Calculation using Eq. 4 gives the following paramagnetic susceptibility, χ_{para}, and Néel temperature, T_N. The susceptibility of the antiferromagnetic region is discussed in Ohya-Nishiguchi's paper:[26]

$$\chi_{para} = \frac{N/2(g\mu)^2}{\kappa|J|+kT\left(1+\exp(|J|/kT)\times\dfrac{\cosh(|J|/kT)}{\cosh(g\mu H/kT)}\right)} \tag{5}$$

$$\exp(-|J|/kT_N)+\cosh(|J|/kT_N) = \kappa\times\sinh(|J|/kT_N), \tag{6}$$

where $\kappa=Z'\times|J'|/|J|$. In the case of $\kappa=0$, χ_{para} is equal to the pair-model susceptibility of Eq. 1. From Eq. 5, it can be seen that χ depends also on the external field, H. At 4.22 K, such a field effect is negligibly small, *i.e.*, $\chi(0)/\chi(0.829\text{ T})=0.98$. By taking the field effect into account, the susceptibility data obtained by the ballistic method in a zero external field were fitted to that obtained by means of a torsion balance in the field of 0.829 T at 4.22 K. A comparison of the theoretical values with the experimental ones shows that the $T_N/T(\chi_{max})$ ratio is best fitted to the experimental one, 0.6, which results in the value of $\kappa=1.3$. The theoretical susceptibility for the case of a single crystal obtained by Ohya-Nishiguchi's model is represented by a dotted

line in Fig. 4 in the case of $\kappa=1.3$; it is qualitatively well fitted to the experimental susceptibility. Using the value of $\kappa=1.3$, the inter-pair interaction $|J'|$ is estimated to be $0.43|J|$ for $Z'=3$ in the case of Fig. 9, while $|J'|=0.26|J|$ is obtained for the case of $Z'=5$ proposed by Duffy *et al.*, who take the other interaction paths into account, also.[11] In both cases, the inter-pair interaction is not so small compared with the intra-pair one.

In conclusion, a spin with antiferromagnetic interaction with a nearest-neighbor spin in free DPPH makes a singlet spin-pair as a ground state. However, in the case of DPPH–Bz spin-pairs interact with each other by means of second-exchange interaction, J', and an antiferromagnetic ordering takes place at a temperature of about 0.40 K. It is difficult, at present, to say definitely what kind of magnetic structure exists in DPPH–$1/4CCl_4$, but it is most likely that DPPH–$1/4CCl_4$ is the case of the coexistence of isolated pairs and mutually interacting pairs.

The author is greatly indebted to Professor Yasuo Deguchi for his continuous help and encouragement. Thanks are also due to Dr. Hiroaki Ohya-Nishiguchi, and Professor Noboru Hirota for their helpful advice and discussions, and to Dr. Toshiaki Enoki and Mr. Toshio Yoshioka for their collaboration. He also wishes to express his appreciation to Professor Ikuji Tsujikawa and Dr. Hanako Kobayashi for their courtesy in carring out the adiabatic demagnetization experiments and for their helpful discussions.

References

1) J. Yamauchi, *Bull. Chem. Soc. Jpn.*, **44**, 2301 (1971).
2) Yu. S. Karimov, *Soviet Phys. JETP*, **30**, 1062 (1970).
3) W. Duffy, Jr., and D. L. Strandburg, *J. Chem. Phys.*, **46**, 456 (1967).
4) M. E. Andereson, G. E. Pake, and T. R. Tuttle, Jr., *J. Chem. Phys.*, **33**, 1581 (1960).
5) Yu. S. Karimov and I. F. Schegolev, *Soviet Phys. JETP*, **13**, 1 (1961).
6) J. A. Weil and J. K. Anderson, *J. Chem. Soc.*, **1965**, 5567.
7) D. E. Williams, *J. Chem. Soc.*, **1965**, 7535; *J. Am. Chem. Soc.*, **89**, 4280 (1967).
8) T. Fujito, T. Enoki, H. Ohya-Nishiguchi, and Y. Deguchi, *Chem. Lett.*, **1972**, 557.
9) C. Th. Kiers, J. L. de Boer, R. Olthof, and A. L. Spek, *Acta Crystallogr., Sect. B*, **32**, 2297 (1976).
10) P. Grobet, L. Van Gerven, and A. Van den Bosch, *J. Chem. Phys.*, **68**, 5225 (1978).
11) W. Duffy, Jr., D. L. Strandburg, and J. F. Deck, *J Chem. Phys.*, **68**, 2097 (1978).
12) P. A. Fedders and J. Kommandeur, *J. Chem. Phys.*, **52**, 2014 (1970).
13) F. Din and A. H. Cockett, "Low-temperature Techniques," George Newnes, London (1960), p. 71.
14) G. B. Benedek and T. Kushida, *Phys. Rev.*, **118**, 46, (1960).
15) B. Bleaney and K. D. Bowers, *Proc. R. Soc. London, Ser. A*, **214**, 451 (1952).
16) R. Verlinden, P. Grobet, and L. Van Gerven, *Chem. Phys. Lett.*, **27**, 535 (1974).
17) T. Yoshioka, H. Ohya-Nishiguchi, and Y. Deguchi, *Bull. Chem. Soc. Jpn.*, **47**, 430 (1974).
18) R. S. Rhodes, J. H. Burgess, and A. S. Edelstein, *Phys. Rev. Lett.*, **6**, 462 (1961).
19) H. Mori, *Bussei*, **1968**, 399.
20) K. Uchino, J. Yamauchi, H. Ohya-Nishiguchi, and Y. Deguchi, *Bull. Chem. Soc. Jpn.*, **47**, 285 (1974).
21) S. Saito and T. Sato, *Phys. Lett. A*, **44**, 347 (1973).
22) R. W. Holmberg, R. Livingston, and W. T. Smith, Jr., *J. Chem. Phys.*, **33**, 541 (1960).
23) A. R. Kessel', B. M. Kozyrev, E. G. Kharakhash'yan, S. Ya. Khelebnikov, and Sh. Z. Shakirov, *JETP. Lett.*, **17**, 453 (1973).
24) A. M. Prokhorov and V. B. Fedrov., *Soviet Phys. JETP.*, **16**, 1489 (1963).
25) T. Oguchi, *Prog. Theor. Phys.*, **13**, 148 (1955).
26) H. Ohya-Nishiguchi, *Bull. Chem. Soc. Jpn.*, **52**, 3480 (1979).